Microbial communities and processes in ice-covered Arctic waters of the northwestern Fram Strait (75 to 80° N) during the vernal pre-bloom phase

Lena Seuthe[1],*, **Birte Töpper[2], Marit Reigstad[1], Runar Thyrhaug[‡],**
Raquel Vaquer-Sunyer[3]

[1]University of Tromsø, Department of Arctic and Marine Biology, 9037 Tromsø, Norway

[2]University of Bergen, Department of Biology, Box 7800, 5020 Bergen, Norway

[3]Department of Global Change Research, IMEDEA (CSIC-UIB), Institut Mediterrani d'Estudis Avançats,
C/Miguel Marqués 21, 07190 Esporles, Mallorca, Spain

ABSTRACT: Marine microbial communities have been little studied in Arctic waters, especially during the winter–spring transition before the development of extensive phytoplankton blooms. This study investigated microbial plankton in the ice-covered polar surface waters of the northwestern Fram Strait (75 to 80°N) at the onset of the 24 h light period in spring (April to May). The system we encountered was characterised by low concentrations of chlorophyll a ($<0.2\ \mu g\ l^{-1}$) and a low abundance of both bacteria (1.4 to 2.5×10^8 cells l^{-1}) and protists (1 to 1.7×10^5 cells l^{-1}). Bacterial production was very low ($\leq 0.63\ \mu g\ C\ l^{-1}\ d^{-1}$), despite the dominance of nucleic-acid-rich bacteria (58 ± 6 % of total bacterial abundance). Small (2 to 5 μm) phototrophs dominated the eukaryotic assemblage in the surface and most probably had profound effects on the composition and metabolic balance of the microbial community as a whole. Most stations appeared to have been net-autotrophic, and calculations of phagotrophy indicated a balanced carbon budget for the microbial community. Mixotrophy was seen in a large part of the ciliate assemblage and may have contributed to the productivity and stability of the pre-bloom system that we encountered.

KEY WORDS: Flow cytometry · Bacteria · Microzooplankton · Mixotrophy · Planktonic metabolism

INTRODUCTION

Microbial communities play a fundamental role in mediating fluxes of carbon and nutrients in marine ecosystems (Azam et al. 1983, Arrigo 2005) by processing a substantial fraction of the pelagic primary production (Cole et al. 1988, Ducklow & Carlson 1992, Calbet & Landry 2004). The dissolved part of the production is readily consumed by bacteria (Cole et al. 1988, Ducklow & Carlson 1992), which, in turn, are preyed upon by small heterotrophic flagellates (Sanders et al. 1992) and, to a lesser extent, by ciliates (Karayanni et al. 2008). Such microbial interactions have been studied extensively in most marine areas, but microbial communities in polar seas have received less attention, perhaps because of the long-prevailing

idea that bacterial growth in polar waters is restricted by low temperatures (Sorokin 1971, Pomeroy & Deibel 1986). Yet, high rates of bacterial production (BP) have been reported from polar seas (e.g. Thingstad & Martinussen 1991, Müller-Niklas & Herndl 1996, Garneau et al. 2008, Sturluson et al. 2008, Rokkan Iversen & Seuthe 2010), and comparative studies from cold- and warm-water oceans show no significant difference in growth rates of bacteria (Rivkin et al. 1996, Kirchman et al. 2005). Consequently, the sparse research conducted on microbial communities in polar waters has revealed the existence of an active (Wheeler et al. 1996) and diverse (Lovejoy et al. 2006) microbial food web. In the Arctic, however, most of the work has been restricted to the productive summer months (e.g. Wheeler et al. 1996, Rich et al. 1997, Sherr et al. 1997),

when ice and weather conditions make it feasible to navigate in ice-covered waters. Little is known about the abundance and trophic structure of microbes during winter and early spring.

The Arctic is characterized by strong seasonality in light, resulting in pronounced changes in photosynthetic production and, consequently, changes in the availability of fresh substrate for the microbial community. Spring appears to be an especially important period in Arctic waters, when the rapidly increasing day length and erosion of sea ice trigger enhanced photosynthetic activity (Sakshaug 2004). Extensive blooms of diatoms are recurrent along the ice edge in spring (von Quillfeldt 1997, 2000), but primary production increases before the phytoplankton cells have accumulated to form a bloom (Behrenfeld 2010). This pre-bloom phase appears to be equally important, allowing the pelagic community to adapt to increasing concentrations of substrate (Yager et al. 2001) and to increasing numbers of prey (Seuthe et al. 2007, Vaqué et al. 2008). The few annual investigations on microbial communities in Arctic waters (Levinsen et al. 2000, Sherr et al. 2003, Garneau et al. 2008, Rokkan Iversen & Seuthe 2011) show major shifts in the composition of the community (Yager et al. 2001, Belzile et al. 2008, Terrado et al. 2008) and in the trophic mode (Alonso-Sáez et al. 2008, Sala et al. 2008, Vaqué et al. 2008) from a net-heterotrophic winter community to vigorous and complex microbial assemblages in spring.

Fram Strait, situated between northeast Greenland and the Svalbard archipelago, connects the Arctic Ocean to the North Atlantic. The strait is the only deep gateway from the central Arctic to adjacent temperate seas, and is thus the site of major water and sea-ice export (Hop et al. 2006 and references therein). Southbound polar water masses, and ice, flow out at the western margin of the strait, following the slope of the northeast Greenlandic shelf in the form of the East Greenland Current (Hop et al. 2006). The exported polar water in the surface layer is characterised by subzero temperatures and salinities <34.7 (Schlichtholz & Houssais 2002). Recirculation of warm, and more saline, modified Atlantic water (>0°C and salinities >34) from the eastern side of the strait is found below the core of the Arctic water (Schlichtholz & Houssais 2002).

The East Greenland Current carries dissolved organic matter (DOM) from the central Arctic Ocean to Fram Strait (Engbrodt & Kattner 2005, Skoog et al. 2005). Much of the DOM in the Arctic Ocean is, however, of terrestrial origin (Anderson 2002) and thus of older and more refractory nature, not easily degraded by marine bacteria. Skoog et al. (2005) suggested that the concentration of bio-reactive, labile DOM in Fram Strait depends heavily on local primary production by both ice algae and phytoplankton. Phytoplankton production in the region appears to be restricted mainly by relatively low concentrations of nitrate, while phosphate and silicate appear to be less limiting (Lara et al. 1994). Most biological investigations of the region have been conducted in the recurrently open waters of the Northeast Water Polynya on the northeast Greenlandic shelf (e.g. Ashjian et al. 1997, Booth & Smith 1997, von Quillfeldt 1997, Pesant et al. 2000), which is characterised by a physical regime somewhat different from that of the East Greenland Current. Further, little work has been conducted on the microbial community in the western part of Fram Strait (but see e.g. Gradinger & Baumann 1991, Auf dem Venne 1994, Gradinger & Lenz 1995).

The main aim of the present study was to describe the microbial pelagic community in ice-covered, Arctic waters at the onset of the productive season. We hypothesised that heavy ice cover should have intercepted the light penetrating into the water column, preventing growth of phototrophs and thus keeping the system in a net-heterotrophic stage. The use of an icebreaker allowed us to penetrate into the heavily ice-covered regions of the northwestern Fram Strait at the beginning of the 24 h light period (April and May 2008). Our data are among the few descriptions of a microbial community during the pre-bloom phase of an Arctic system in early spring.

MATERIALS AND METHODS

Sampling. The investigation took place in the northwestern Fram Strait using the Norwegian coastguard icebreaker KV 'Svalbard' between April 22 and May 27, 2008. A total of 6 stations between 74.9 and 79.6°N and between 2.4 and 13.4°W were sampled; the 3 southernmost stations (Stns C1, D, E) were sampled first (Fig. 1). Thus, although the stations are labelled essentially from north to south (Stns A, B, C2, C1, D, E) they were sampled in a different temporal sequence (C1, D, E, A, B, C2). In the figures, stations are sorted according to their temporal order. All stations were situated on the northeast Greenlandic shelf or along its seaward slope. Station depths ranged between 260 and 2600 m. All stations were ice-covered (40 to 100%). Water characteristics such as temperature, salinity and density were measured using a Seabird SBE 9.11+ lowered to the bottom (data at depths >200 m are not shown).

Incident radiation was measured throughout the upper 80 to 100 m of the water column with two TriOS Ramses ACC sensors, measuring spectral flux from the near-ultraviolet to the near-infrared with a spectral resolution of about 3.3 nm. One sensor was mounted
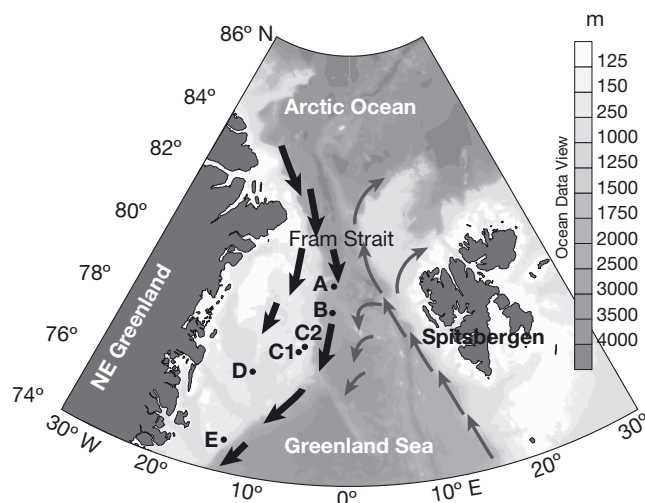
Fig. 1. Area investigated and sampling sites along the northeast Greenlandic shelf. The East Greenland Current (thick black arrows) follows the shelf topography, exporting large quantities of polar water and sea-ice from the central Arctic Ocean. Warm Atlantic water (thin grey arrows) is transported northwards along the western side of Spitsbergen and is partly recirculated within Fram Strait

and leveled on the helicopter deck, above most of the objects on the ship, in order to minimise shadowing; this sensor measured incoming light. A second sensor was placed in a frame and deployed over the side of the ship on which the sun was shining; this sensor measured transmitted light. The latter was steadily lowered at about 0.5 m s^{-1}, and measurements were made from both sensors as frequently as the integration time for the underwater sensor allowed (about every second near the surface, every 5 s near the bottom). The spectral fluxes were integrated from 400 to 700 nm to get photosynthetically active radiation (PAR) fluxes, and the PAR flux measured at depth was divided by the PAR flux measured at the same time at the surface. The euphotic zone was defined as the depth at which 0.1% of surface radiation was measured.

Water was sampled with Niskin bottles from 7 discrete depths (1, 5, 10, 20, 30, 40 and 50 m) for analyses of inorganic nutrients, particulate organic carbon (POC), chlorophyll a (chl a), bacterial abundance (BA) and BP, as well as nanoplankton and microplankton (the latter 2 were not analysed in samples from 1 m). For measurement of nutrients (phosphate, nitrate and nitrite), subsamples of water were frozen and later analysed with standard seawater methods applying a Flow Solution IV analyzer (OI Analytical), calibrated using reference seawater (Ocean Scientific International). For analyses of POC, triplicate subsamples (500 to 1000 ml) were filtered on pre-combusted Whatman GF/F glass fibre filters (450°C for 5 h), dried at 60°C for 24 h and analysed on shore with a Leeman Lab CEC

440 CHN analyzer after removal of carbonate by fuming with concentrated HCl for 24 h. For total chl a, triplicate subsamples (150 to 500 ml) were filtered through Whatman GF/F glass-fibre filters. The filters were analysed fluorometrically (10-AU, Turner Designs) after extraction in 5 ml methanol at room temperature in the dark for 12 h without grinding. All biological and chemical data processed from discrete water samples were integrated for the upper 60 m of the water column using trapezoidal integration.

Abundance and production of heterotrophic prokaryotes. The total number of heterotrophic prokaryotes was determined using a FACSCalibur flow cytometer (Becton Dickinson) equipped with an air-cooled laser providing 15 mW at 488 nm with a standard filter setup. The cells were fixed with glutaraldehyde (final conc. 0.5%) for 30 min at 4°C and stored in liquid nitrogen until further analysis. Appropriate dilutions of fixed samples were prepared (2- to 5-fold) in 0.2 µm filtered TE buffer and stained with a green fluorescent nucleic-acid dye (SYBR Green I, Invitrogen) for 10 min at room temperature in the dark. The samples were analysed for 1 min at a flow rate of approx. 50 µl min^{-1} with the discriminator set on green fluorescence. Determination of the prokaryote population was based on scatter plot observations of the light side-scatter signal (SSC) versus the green fluorescence signal of SYBR Green I (FL). Two subgroups of prokaryotes were discriminated on the basis of their different levels of FL signal. The group with the stronger FL signature (denoting high levels of nucleic acid) is hereafter called HNA bacteria, and the other group (with low levels of nucleic acid) is called LNA bacteria. The cell numbers were calculated from the instrument flow rate based on volumetric measurements. Prokaryote abundance was converted to biomass by a carbon-conversion factor of 20 fg C cell^{-1} (Lee & Fuhrman 1987).

Arctic surface waters appear to be dominated by bacteria (Wells & Deming 2003), with *Crenarchaeota* (members of the domain *Archaea*) representing only about 10% of prokaryotes in surface waters shallower than 100 m (Kirchman et al. 2007). Heterotrophic prokaryotes will therefore be called bacteria hereafter.

BP was measured by incorporation of ^{3}H-leucine (specific activity: 4.27 TBq mmol^{-1}) according to Smith & Azam (1992). A sample volume of 1.5 ml was incubated with ^{3}H-leucine (final conc. 40 nM) for exactly 1 h at 4°C in the dark. The incubation was terminated by adding trichloroacetic acid (TCA; final conc. 5%). The control received the same amount of TCA before starting the incubation. The fixed samples were stored at 4°C until further analysis. The samples were then centrifuged (10 min, 20 400 × g) and the supernatants removed. The pellets were washed 2

times by adding 1 ml of 5% TCA followed by centrifuging (10 min, $20\,400 \times g$). After removing the supernatant, 1 ml of liquid scintillation cocktail (Ecosint A, National Diagnostics) was added to the pellet and mixed well. The samples were radioassayed in a liquid scintillation counter (Perkin Elmer). Leucine incorporation was converted into biomass production using the carbon fraction of proteins of 1.5 (Simon & Azam 1989, Ducklow 2003 and references therein).

Biomass and taxonomic composition of protozooplankton. Flagellates were fixed with glutaraldehyde (1% final conc.) before 200 ml of the sample was filtered through black polycarbonate filters (pore size 0.8 µm) and stained with 4,6-diamidino-2-phenylindole dihydrochloride (DAPI) (Porter & Feig 1980) at $5\,\mu g\,l^{-1}$. The filters were mounted on microscope slides and subsequently frozen at –20°C to preserve the chlorophyll autofluorescence (Porter & Feig 1980, Bloem et al. 1986, Sanders et al. 1989). The samples were counted under an epifluorescence microscope (Nikon Elipse TE300) at 400× magnification, using ultraviolet and green excitation to identify emission from DAPI and chl *a*, respectively. Each sample was counted 3 times, with 20 grids being counted on the filter. The final cell abundance was calculated as the average cell abundance retrieved from the 3 counts. Cells were divided into 3 size groups (2 to 5 µm, 5 to 10 µm, and >10 µm) for both phototrophic flagellates (PF) and heterotrophic flagellates (HF). Cells that were <2 µm, but clearly flagellates, were included in the size class 2 to 5 µm. The biomass of PF and HF was calculated from biovolume estimates and the application of a carbon conversion factor of pg C cell^{-1} = $0.216 \times$ vol$^{0.939}$ (Menden-Deuer & Lessard 2000). Flagellate biovolume was estimated for the different size groups by using the average group size as the diameter of a sphere.

Samples for ciliate and dinoflagellate identification and enumeration (1 l) were fixed with acid Lugol (2% final conc.). The samples were stored in a cool dark place, and allowed to settle in a large glass cylinder for 48 h, before the supernatant was carefully removed by inverse gravitational filtration (mesh size 10 µm). The concentrate (100 ml) was allowed to settle in an Utermöhl sedimentation chamber, and the entire chamber was examined under an inverted microscope (Leitz DM IL) at a magnification of 200×. Cell sizes of at least 30 specimens of each species or type of cell were measured with the help of a graticule. Standard geometric forms were used to determine the cell volume from length and width measurements. The biovolume was converted to biomass using a volume-to-carbon conversion factor of 0.19 pg C µm^{-3} (Putt & Stoecker 1989) for aloricate ciliates. For dinoflagellates we used a carbon conversion factor of pg C cell^{-1} = $0.76 \times$ vol$^{0.819}$

(Menden-Deuer & Lessard 2000). Ciliates were divided, independently of cell size, into the functional groups of heterotrophs (*Leegaardiella* sp., *Lohmanniella* sp., *Strombidium* spp. and *Strobilidium* sp.), the mixotrophs *Laboea strobila* and *Strombidium conicum* (Stoecker & Michaels 1991), and the functionally phototrophic *Mesodinium rubrum* (Hansen & Fenchel 2006). Dinoflagellates >20 µm were added to the flagellate size group >10 µm, counted from the DAPI-stained samples. The flagellate group >10 µm consequently includes cells counted from DAPI and acid Lugol samples.

Community metabolism. Planktonic community metabolism was evaluated from changes in oxygen concentration in narrow-mouth Winkler bottles. Incubation water was sampled with the CTD rosette from 1, 5, 10 and 20 m and directly siphoned over into incubation bottles. Six bottles from each depth were fixed inmediately for determination of the initial oxygen content. The other bottles (6 clear bottles and 6 dark bottles for each depth) were incubated *in situ* at the respective depths of 1, 5, 10 and 20 m, hanging attached to the edge of an ice-floe. The bottles were thus exposed to natural light and temperature conditions over the course of the 24 h incubation. However, this form of incubation led to the loss of bottles and whole rigs at some of the stations owing to heavy ice-scoring. Upon retrieval, the dissolved oxygen concentration was measured by high-precision Winkler titration, using a precise automated titration system with potentiometric (redox electrode) end-point detection (Mettler Toledo DL28 titrator), following the recommendations of Carritt & Carpenter (1996).

Community respiration rates (CRs) were calculated from the difference between the initial oxygen concentration and the oxygen concentration in the dark bottles after incubation for 24 h. Net community production (NCP) was calculated from the difference between the oxygen concentration in the clear bottles after incubation and the initial oxygen concentration. Gross primary production (GPP) was calculated as the sum of NCP and CR.

Depth-integrated (0 to 20 m) metabolic rates were calculated for each station. Where needed, the data were converted to carbon units, assuming a 1.25 molar stoichiometry between oxygen and carbon (Williams et al. 1979).

Treatment of data. The relationships between 2 biological variables were examined by means of regression analyses, computing Linear Least Squares (OLS) statistics (Systat$^{©}$ 13). Differences in POC, chl *a*, and microbe abundance between stations and depths were tested with factorial analysis of variance (ANOVA), after log-transformation of the data to satisfy assumptions of normality. Parameters for which no statistically

significant difference was recorded between stations (level of significance: 0.05) are indicated by box plots underlying the original abundance profiles, giving the mean and the 25 and 75% percentiles of the data. A multiple linear regression analysis was conducted to asses which factors (salinity, temperature, concentrations of chl *a* and POC, abundance of phototrophic and heterotrophic protists) were most important for explaining BA. All abundance data were log-transformed prior to the analysis to correct for non-normal distributions. In the multiple regression analysis, the most significant variables explaining the observed variance in log-transformed BA were identified by backward elimination (SYSTAT© 13), i.e. all potential explanatory variables were initially included and tested for significance at the 5% level.

Calculations of potential protist grazing and production. Daily protozoan production was calculated from the respective biomasses of HF and ciliates multi- plied by a growth rate (μ) of $\ln(\mu) = 0.1 \times t - 1$ at the measured *in situ* temperatures (t), according to Rose & Caron (2007) for herbivorous protists. Protozoa appear incapable of achieving maximal growth at low food concentrations, and their growth rate was thus assumed to be half their maximal growth rate μ at the given temperature, as suggested by Sherr & Sherr (2009) for food concentrations <5 µg chl *a* l^{-1}. Ingestion by the heterotrophic part of the protozoan assemblage was calculated from the production rate, assuming a growth efficiency of 33% (Hansen et al. 1997). The daily carbon demands of the bacterial community were calculated from the measured average BP, assuming a growth efficiency of 33% (del Giorgio & Cole 1998).

RESULTS

Physical regime, nutrients, and chl *a*

All stations had ice cover consisting predominantly of first-year sea ice. Stns C1, E, A and B were, on average, >80% covered with ice, while Stns D and C2 had <60% ice cover (S. Hudson pers. comm.). However, the ice cover changed — often rapidly — during the course of a day. This was especially true for Stns D and C2 where ice coverage varied between 15 and 60% within 24 h. The euphotic zone

ranged between 50 and 70 m in depth in open waters between the ice floes (Table 1). At all stations, the surface water (0 to 60 m) was cold (–1.8 to –1.5°C) with reduced salinity (32.13 to 34.24). Warmer and more saline (temperature >0°C and salinity >34) water of Atlantic origin was found at depths >100 m at most stations (Fig. 2). Average concentrations of nitrogen (nitrate and nitrite) ranged between 3.6 and 7.7 µM, and average concentrations of phosphate ranged between 0.4 and 0.5 µM (Table 1).

Table 1. Integrated (0 to 60 m) values (mg C m^{-2}) of chlorophyll *a* (chl *a*), particulate organic carbon (POC), bacteria biomass (BB), biomass of different size classes of phototrophic flagellates (PF) and heterotrophic flagellates (HF), mixotrophic (Mix.) and heterotrophic (Het.) ciliates, as well as the phototrophic ciliate *Mesodinium rubrum* at the 6 stations in Fram Strait. The class 'Total phago. ciliates' contains both heterotrophic and mixotrophic forms. Two biomass ratios are given, with H$_{protist}$:P being the ratio of heterotrophic (total HF + phagotrophic ciliates) versus phototrophic protists (total PF + *M. rubrum*), and H$_{protist+bacteria}$:P being the total heterotrophic biomass (total HF + phagotrophic ciliates + bacteria) divided by phototrophic protist biomass. Community metabolic rates, such as net community production (NCP), community respiration (CR), and gross primary production (GPP) are given in mmol O$_2$ m^{-2} d^{-1}, integrated from surface to 20 m. Depth (m) of the euphotic zone (here defined as 0.1% incident photosynthetically active radiation), and average concentrations of nitrogen (nitrate and nitrite) and phosphate (µM) are given. bd: below detection limit of the method used. nd: no data

|			Stn			
	C1	D	E	A	B	C2
Euphotic zone	60	50	70	50	70	60
Nitrogen	3.6	4.9	7.7	7.2	7.6	4.5
Phosphate	0.5	0.4	0.5	0.5	0.5	nd
POC	2674.3	1559.3	1955.6	2126.8	2160.2	1693.8
Chl *a*	4.6	2.7	9.5	5.6	11.5	7.0
Community metabolism						
NCP	35.1	88.8	–3.5	nd	nd	nd
CR	bd	bd	19.2	nd	nd	nd
GPP	bd	bd	18.1	nd	nd	nd
Bacteria						
BB	289.7	181.3	202.4	172.7	302.2	245.0
Flagellates						
PF 2–5 µm	6.3	6.4	7.1	5.0	9.2	5.0
PF 5–10 µm	8.5	6.2	12.1	10.6	17.1	8.1
PF >10 µm	23.1	18.8	38.5	43.3	68.8	50.8
Total PF	37.8	31.4	57.8	58.9	95.1	63.8
HF 2–5 µm	6.2	6.2	5.6	5.8	8.4	6.1
HF 5–10 µm	1.0	0.8	1.6	2.0	3.7	2.8
HF >10 µm	13.2	6.4	6.4	17.4	8.5	16.0
Total HF	20.3	13.4	13.6	25.2	20.5	24.8
Ciliates						
M. rubrum	15.1	16.6	22.8	20.9	16.8	22.3
Mix. ciliates	15.4	13.6	62.8	56.8	23.7	11.6
Het. ciliates	9.0	13.1	16.1	8.7	18.2	10.8
Total phago. ciliates	24.4	26.6	78.9	65.5	41.9	22.3
Biomass ratios						
H$_{protist}$:P	0.8	0.8	1.1	1.1	0.6	0.5
H$_{protist+bacteria}$:P	6.3	4.4	3.7	3.3	3.3	3.4
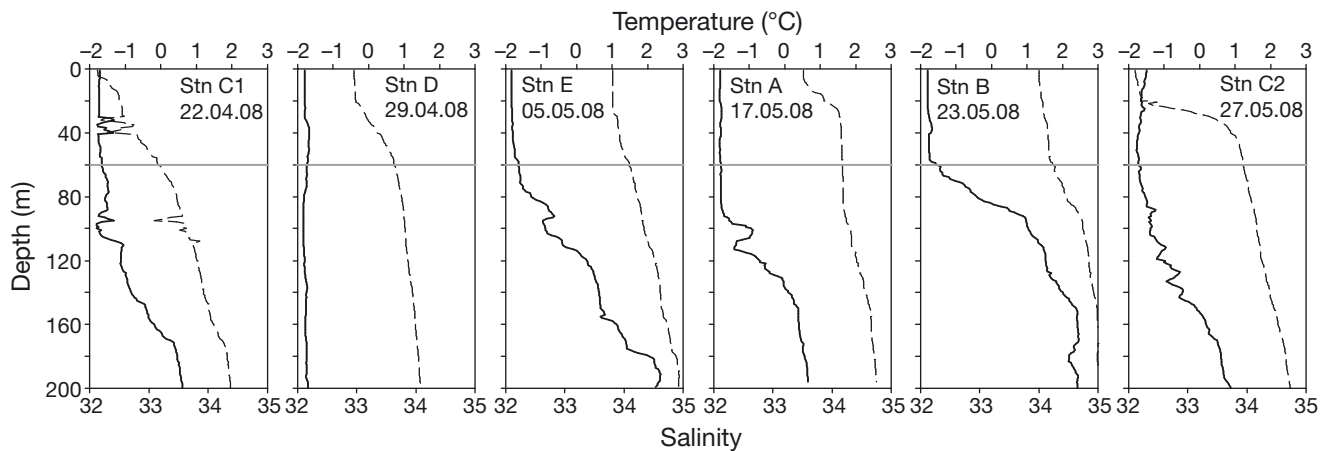
Fig. 2. Water temperature (solid line) and salinity (broken line) over the upper 200 m at the 6 sampling stations. Horizontal grey line marks 60 m depth, to which biological samples were taken. Dates are given as dd.mm.yy

The integrated phytoplankton biomass, represented as standing stock of chl a in the upper 60 m, remained low throughout the period of investigation (2.7 to 11.5 mg chl a m^{-2}, Table 1), but concentrations of chl a differed significantly between stations (ANOVA, F = 6.456, p < 0.001). The highest concentrations of chl a were encountered at Stns E and B, while Stns D and C1 had the lowest concentrations. The variance in chl a was not explained by the ice cover recorded at the respective stations (OLS, r^2 = 0.083, $F_{1,4}$ = 0.364, p = 0.579, n = 36). Also, the integrated biomasses of POC differed significantly between stations (ANOVA, F = 4.541, p = 0.003), ranging from 1515 to 2637 mg C m^{-2}, with the highest concentration at Stns C1 and E, and the lowest at Stns D and C2 (Table 1). Thus, chl a explained little of the variance observed in POC (OLS, r^2 = 0.116, $F_{1,34}$ = 4.47, p = 0.042, n = 36).

Abundance of microbes and bacterial production

BA was positively correlated with the concentration of chl a ($Y_{\log BA}$ = 0.759 $X_{chl\ a}$ + 8.186; r^2 = 0.218, $F_{1,34}$ = 10.765, p = 0.002, n = 36) and POC ($Y_{\log BA}$ = 0.07 X_{POC} + 8.047; r^2 = 0.250, $F_{1,34}$ = 12.697, p = 0.001, n = 36). Multiple linear regression with backward elimination found the combined effect of chl a and temperature to be the best explanation of log-transformed BA ($Y_{\log BA}$ = 9.015 + 0.845 $X_{chl\ a}$ + 0.485 $X_{temperature}$; r^2 = 0.458, $F_{2,33}$ = 15.796, p < 0.001, n = 36). As indicated by the relative size of the partial regression coefficient of chl a, the concentration of chl a had the strongest influence on the bacterial stocks.

Bacterial concentrations remained constant over depth (ANOVA, p > 0.05; Fig. 3A), but differed between stations (ANOVA, F = 25.181, p < 0.001), with

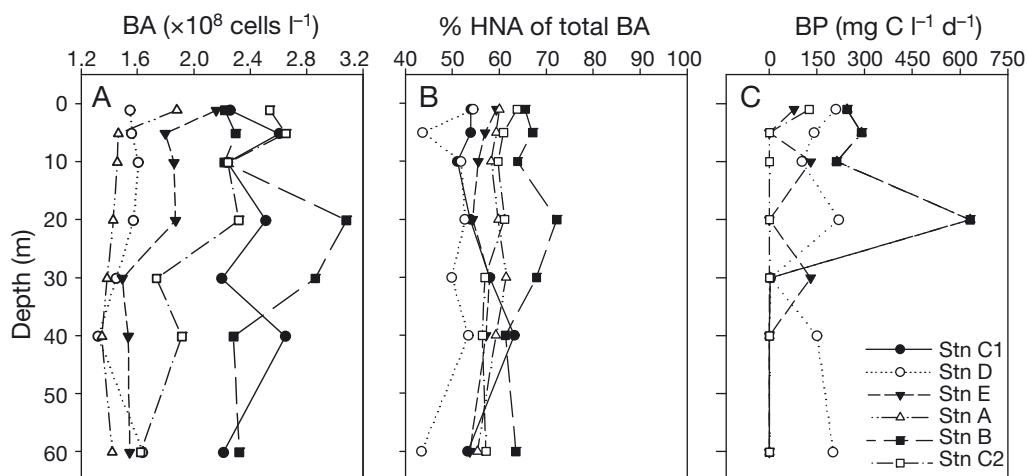Fig. 3. (A) Bacterial abundance (BA, cells × 10^8 l^{-1}), (B) contribution of high-level nucleic acid (HNA) bacteria to total BA (%), and (C) bacterial production (BP) in the upper 60 m of the water column for the respective stations. BP rates were below the detection limit of the method at many depths and are presented as zero here

Stns C2, C1 and B having the highest average BA (2.1 to 2.5×10^8 cells l^{-1}) in the upper 60 m, while Stns A, D and E had the lowest (1.4 to 1.7×10^8 cells l^{-1}). The bacterial community was characterised by a strong FL signal from the nucleic-acid-bound SBYR Green I stain and a strong SSC. HNA bacteria dominated the bacterial assemblage numerically, constituting on average $58 \pm 6\%$ (Fig. 3B). HNA bacteria contributed most to the total BA at Stn B ($66 \pm 4\%$) and least at Stn D ($50 \pm 5\%$).

BP rates were so low that they were close to, or below, the detection limit of the method (Fig. 3C). Where detected, BP rates ranged between 2 and 628 mg C l^{-1} d^{-1}. The non-detection of BP at many depths precluded depth integration at most stations, but Stns C1 and B yielded 8.4 and 9.7 mg C m^{-2} d^{-1}, respectively, for the upper 60 m.

The abundance of PF (2 to >10 μm) explained 50% of the variance in concentration of chl a (OLS, $r^2 = 0.485$, $F_{1,34} = 31.995$, p < 0.001, n = 36). Both PF and HF were present at a total average abundance of 1.06 to 1.67×10^5 cells l^{-1} throughout the upper 60 m of the water column, with increased concentrations towards the surface layer (Fig. 4). PF were more abundant than HF in the upper 30 m. Both PF and HF were dominated by cells in the size class 2 to 5 μm, which constituted >80% in terms of numbers (Fig. 4A,D). We found a smaller fraction (8 to 17%) of PF in the size class 5 to 10 μm, while the number of HF >5 μm contributed only <6% to the total abundance. The variance observed in the abundance of HF (2 to >10 μm) was explained to 45% by the abundance of PF (2 to >10 μm; OLS, $r^2 = 0.452$, $F_{1,34} = 28.058$, p <
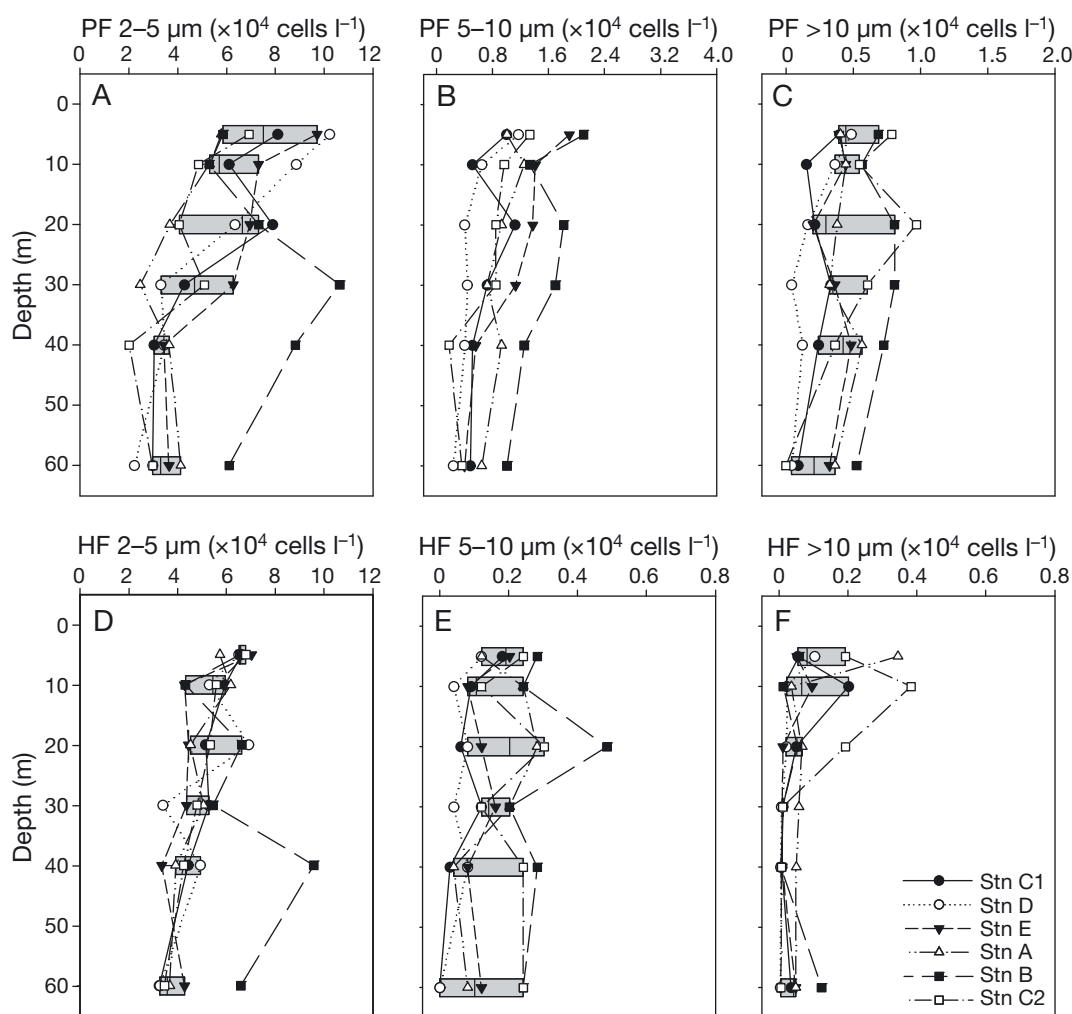

Fig. 4. Abundance of 3 size groups (2 to 5, 5 to 10, and >10 μm) of (A–C) phototrophic flagellates (PF) and (D–F) heterotrophic flagellates (HF) in the upper 60 m of the water column for the respective stations. The underlying grey box-plots indicate the 25 and 75% percentiles and mean of the 6 stations, where stations did not differ significantly from each other (ANOVA, p > 0.05). Only profiles of PF 5 to 10 μm were significantly different from each other at the 6 stations (ANOVA, $F = 3.81$, p = 0.01). All profiles showed significant differences with depth (ANOVA, p < 0.05)

0.001, n = 36), while BA explained only 18% (OLS, $r^2 = 0.175$, $F_{1,34} = 7.218$, p = 0.011, n = 36) of the abundance of HF (2 to >10 µm).

The abundance of ciliates ranged between 98 and 642 cells l^{-1} (Fig. 5). The phototrophic species *Mesodinium rubrum* dominated the ciliate community in terms of numbers, with up to 424 cells l^{-1}, while heterotrophic and mixotrophic forms did not reach an abundance higher than 150 cells l^{-1} and 100 cells l^{-1}, respectively. Mixotrophic ciliates contributed, on average, 31% to the total of phagotrophic ciliates (i.e. heterotrophic and mixotrophic ciliates). The abundance of PF in the size class 2 to 10 µm explained 28% of the variance in abundance of phagotrophic ciliates (OLS, $r^2 = 0.283$, $F_{1,34} = 13.447$, p = 0.001, n = 36), while BA was not significantly correlated to the abundance of either phagotrophic or heterotrophic ciliates (OLS, p > 0.05).

The abundance of most protists did not differ significantly between stations (ANOVA, p > 0.05), despite differences in profile curvatures. Exceptions were the profiles of PF 5 to 10 µm (Fig. 4B) and heterotrophic ciliates (Fig. 5C). Due to the similarity of most protist profiles, the data from the different stations will be discussed as variations of the same biological state of the system.

Microbial biomasses

Integrated bacterial biomass equalled (Stns A and E) or exceeded the total biomass of protists by a factor of 1.7 to 3, ranging between 173 and 302 mg C m^{-2} for the upper 60 m of the water column (Table 1). PF biomass, ranging from 31 to 95 mg C m^{-2}, was dominated by cells >10 µm. The integrated biomass of HF varied between 13 and 25 mg C m^{-2} and was thus only 18 to 35% of the total flagellate biomass. Among HF, small (2 to 5 µm) and large (>10 µm) cells contributed more evenly to the total biomass than they did among PF. The biomass of ciliates was dominated by chloroplast-bearing forms, such as *Mesodinium rubrum* and the obligate mixotrophs *Laboea strobila* and *Strombidium conicum*. The biomass of *M. rubrum* was of the same order of magnitude as that of HF, ranging from 15 to 23 mg C m^{-2}. Mixotrophic ciliates reached biomasses of up to 63 mg C m^{-2}, while heterotrophic ciliate biomass did not exceed 18 mg C m^{-2}. Consequently, the biomass of protists was dominated by phototrophic forms at most stations ($H_{protist}$:P < 1; Table 1).

Plankton community metabolism

Ice-scoring led to the loss of incubation rigs, and we were able to determine planktonic metabolism at only 3 of the 6 stations (Table 1). At 2 of the 3 stations, 20 m integrated NCP was positive, 35.1 ± 7.8 and 88.8 ± 8.6 mmol O_2 m^{-2} d^{-1}, indicating net autotrophy. Concurrently, the biomass ratio of heterotrophic to phototrophic protists, $H_{protist}$:P, was 0.8 at these net autotrophic stations. At Stn E, $H_{protist}$:P was 1.1, coinciding with a CR of 19.2 ± 7.0 mmol O_2 m^{-2} d^{-1}, which was higher than the GPP rate (18.1 ± 12.3 mmol O_2 m^{-2} d^{-1}). This resulted in a slightly negative NCP (–3.5 ± 10.1 mmol O_2 m^{-2} d^{-1}), and, consequently, net heterotrophy of the encountered system.
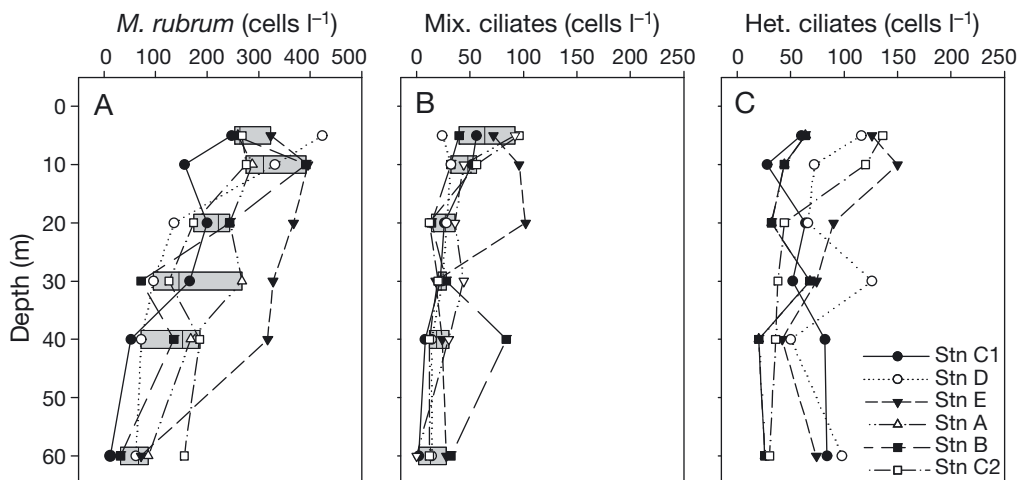

Fig. 5. Abundance of (A) the functionally phototrophic ciliate *Mesodinium rubrum*, (B) mixotrophic (Mix.) ciliates, and (C) heterotrophic (Het.) ciliates in the upper 60 m of the water column for the respective stations. The underlying grey box-plots are explained in the legend of Fig. 4. Only profiles of heterotrophic ciliates were significantly different from each other at the 6 stations (ANOVA, F = 3.46, p = 0.01). All profiles showed significant differences with depth (ANOVA, p < 0.05)

DISCUSSION

Early spring stage of an Arctic marine ecosystem: community and trophic status

The present study took place in the Arctic surface waters of the East Greenland Current at the beginning of the midnight sun (24 h light) period in spring. Virtually all groups of microbes were present in the upper 60 m of the water column, despite heavy ice cover, persistently low water temperatures, and low concentrations of chl *a*. Among protists, phototrophic forms dominated in terms of both number and biomass ($H_{protist}:P \leq 1$). The dominance of phototrophic protists indicated that the microbial food web encountered in Fram Strait had turned from a winter to an early spring stage.

Phototrophic cells occurred in low numbers, compared to open-water and summer situations in the Arctic (e.g. Booth & Smith 1997, Sherr et al. 2003, Tremblay et al. 2009). Their abundance was, however, comparable to those reported previously from other ice-covered Arctic waters during winter and early spring (Table 2). As for other Arctic ecosystems early in the season (Sherr et al. 2003, Lovejoy et al. 2007), the phototrophic community in Fram Strait was dominated by small flagellates (1.5 to 3 μm), most probably *Micromonas*-like prasinophytes. These flagellates have been found to maintain bright fluorescence during winter and to start to increase in population, below ice, at approx. 70°N from as early as February onwards (Lovejoy et al. 2007, Terrado et al. 2008). Relatively high growth rates of these small flagellates under low-light conditions (Lovejoy et al. 2007) may be the reason why they are found to dominate Arctic late-winter and early-spring assemblages, as seen also in the present study. Diatoms, on the other hand, which are characteristic for ice-algae assemblages (Rozanska et al. 2009) and pelagic ice-edge blooms (von Quillfeldt 1997, 2000), were observed only in low numbers (of the order of 10^1 to 10^2 cells l⁻¹, data not shown), indicating that a pre-bloom stage prevailed in the system we encountered.

Net community oxygen measurements supported the view that the system in Fram Strait had turned from a wintry net heterotrophic to a net autotrophic stage. Two out of 3 stations were net autotrophic (NCP > 1; Table 1). At these stations, phototrophic protist biomass

Table 2. Comparison of winter and pre-bloom spring data from polar and sub-polar regions. Ranges or averages of chlorophyll *a* concentrations (chl *a*, μg l⁻¹), bacterial production (BP, μg C l⁻¹ d⁻¹), as well as bacterial abundance (BA, cells × 10⁸ l⁻¹), heterotrophic flagellates (HF) and phototrophic flagellates (PF) (in cells × 10⁵ l⁻¹), and ciliates (Cil, cells × 10³ l⁻¹). D: depth (m) of the investigated surface layer

Area	Season	Chl a	BP	BA	HF	PF	Cil	D	Source
Arctic Ocean	Nov–May	<0.2	<0.01–0.06	1.32–2.86	0.9–4.9	0.03–15	3.0–9.7[a]	40 50	Sherr et al. (2003) Sherr & Sherr (2003)
SE Beaufort Sea	Dec–Mar Apr–May	0.04–0.15 0.20–0.36		1.74–3.39 1.49–5.16	1.88–7.55 2.21–6.45	0.28–1.53 1.64–4.54	0.09–1.28 0.18–1.29	0	Vaqué et al. (2008)
SE Beaufort Sea	Feb–Mar Apr–May	<0.2 <0.4	<0.03 <0.16	<4 <5				250	Garneau et al. (2008)
SE Beaufort Sea	Dec–Mar Apr–May			2.4 2.7	1 1.57	0.34 0.74		0	Terrado et al. (2008)
W Greenland	Nov–Mar	0.2					0.25	200	Levinsen et al. (2000)
W Spitsbergen	Dec Mar	<0.03 0.01–0.02	0.1–0.56 0.36–1.41	2.58–2.97 1.76–2.09	0.43–0.94 0.04–0.45	0.03–0.17 0.13–0.48	0.09–0.21 0.09–0.57	50	Rokkan Iversen & Seuthe (2011) Seuthe et al. (2011)
NW Fram Strait	Apr–May	0.01–0.25	≤0.63	1.33–3.09	0.33–0.99	0.24–1.31	0.1–0.64	60	Present study

[a]Heterotrophic protists 20–200 μm

dominated over that of heterotrophic protists ($H_{protist}$:P < 1; Table 1), suggesting that the metabolic rates of the protists had a strong influence on the communities' metabolic balance. Bacterial respiration appeared to have had little influence on the communities' trophic stage, as indicated by the very low rates of BP. Integrated BP was, on average, only 5% of the integrated GPP (Fig. 6), despite bacterial numbers being within the range described previously from a variety of Arctic marine ecosystems (Müller-Niklas & Herndl 1996, Sturluson et al. 2008, our Table 2). The presence of relatively large HNA bacteria resulted in a high bacterial biomass, which caused the total heterotrophic biomass (biomass of bacteria and heterotrophic protists) to greatly exceed that of phototrophs at all stations ($H_{protist+bacteria}$:P >> 1; Table 1). Such dominance of heterotrophic over phototrophic biomass has been found

Fig. 6. Carbon budget for the integrated stocks of microbes (boxes, mg C m^{-2}) averaged for the 6 stations (±SD). Vertical arrows indicate calculated production rates (mg C m^{-2} d^{-1}). For bacteria, the vertical arrow represents bacterial production (mg C m^{-2} d^{-1}), as measured by incorporation of radiolabelled leucine. The value on gross primary production (vertical arrow on the phototrophic side, mg C m^{-2} d^{-1}) stems from measurements of O$_2$ production. Inclined arrows indicate calculated daily carbon demands (mg C m^{-2} d^{-1}), assuming a growth efficiency of 0.33 for bacteria (del Giorgio & Cole 1998) and heterotrophic protists (Hansen et al. 1997). PF: phototrophic flagellates; HF: heterotrophic flagellates; Phot. cil.: phototrophic ciliates (*Mesodinium rubrum*); Mix. cil.: mixotrophic ciliates; Het. cil.: Heterotrophic ciliates

characteristic for open-ocean, low-chlorophyll environments (Gasol et al. 1997). These systems have been shown to be governed by higher phototrophic turnover rates than heterotrophic ones (Gasol et al. 1997), due to the prevalence of fast-growing, small phytoplankton (Agawin et al. 2000). Similarly, the planktonic prebloom system encountered in Fram Strait appeared metabolically driven by small phototrophs, despite the presence of inverted biomass pyramids dominated by heterotrophs, and bacteria in particular.

Bacterial spring community consisted of large, nucleic-acid-rich cells

The bacterial assemblage encountered in Fram Strait resembled bacterial spring communities described from other Arctic regions, both in total BA (Table 2) and in dominance of HNA bacteria. Belzile et al. (2008) found that the fraction of HNA bacteria dominated as bacterial numbers started to increase in spring (April), after having constituted a minor fraction during winter under the land-fast ice of the southeastern Beaufort Sea. The dominance of HNA bacteria found in the present study is thus a further indication that the microbial community in Fram Strait had turned from a winter stage into a spring pre-bloom stage.

In the Beaufort Sea, the increase in BA, and the shift towards HNA bacteria (Belzile et al. 2008), was accompanied by enhanced BP (Garneau et al. 2008). In Fram Strait, cell-specific BP rates (BP/BA) were of the same order of magnitude (1.5×10^{-11} to 1.1×10^{-9} µg C cell^{-1} d^{-1}) as in the Beaufort Sea (7.5×10^{-11} µg C cell^{-1} d^{-1} (Garneau et al. 2008). These rates are low compared to those reported from polar bacterial assemblages during summer, which range from 6.8×10^{-10} µg C cell^{-1} d^{-1} (Howard-Jones et al. 2002) to 1.5×10^{-8} µg C cell^{-1} d^{-1} (Sturluson et al. 2008). Nevertheless, our measurements gave significantly higher numbers than those reported from the central Arctic Ocean during winter (1.1×10^{-13} µg C cell^{-1} d^{-1}, Sherr & Sherr 2003), indicating that BP in Fram Strait most probably had increased from its wintry background level.

Arctic marine bacteria are thought to experience strong grazing pressure from a starving heterotroph community during the dark months of the polar winter (Anderson & Rivkin 2001, Vaqué et al. 2008). It is not until the return of the light and slight increases in chl *a* that bacterial numbers rise (Sherr et al. 2003, Belzile et al. 2008). As a mechanism behind this numerical increase in spring, Anderson & Rivkin (2001) suggested that the grazing pressure on bacteria is released when picophytoplankton become abundant in early spring, serving as an alternative and potentially more nutritious source of food for the heterotrophs. In Fram Strait, this
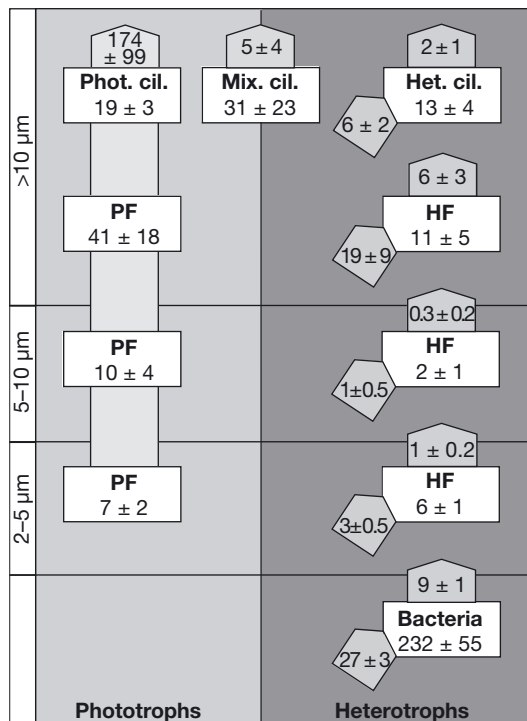
notion seemed to be supported by the finding that PF explained 45%, while bacteria explained only 18% of the variance observed in HF numbers. Also, the abundance of heterotrophic ciliates could partly be explained by small phototrophs (2 to 10 μm), but not by bacteria. It is thus reasonable to assume that the bacterial community in Fram Strait experienced a reduced grazing pressure due to the presence of small phototrophs.

Vaqué et al. (2008) found that the bacterial assemblage under the ice in the Beaufort Sea became substrate limited as grazing pressure on the bacterial community relaxed in early spring. In Fram Strait, mineral nutrients, such as nitrogen and phosphate, were present at concentrations not known to limit bacterial growth. Further, measurements of GPP suggest the presence of freshly produced dissolved organic carbon because a fraction of the daily production of 174 ± 99 mg C m^{-2} d^{-1} must have been in the form of extracellular, dissolved carbon. Vernet et al. (1998) reported that the fraction of extracellular primary production in ice-covered waters of the Barents Sea was in the range 18 to 55% of the total production under phytoplankton bloom conditions. In Fram Strait, the daily production of extracellular carbon may consequently have ranged between 31 and 96 mg C m^{-2} d^{-1}, and thus may have been sufficient to cover the presumed carbon demands of bacteria (Fig. 6). On the other hand, extracellular primary production may increase with nutrient limitation and may be sensitive to species composition (Vernet et al. 1998). We cannot exclude the possibility that extracellular primary production accounted for a far smaller fraction under the nutrient-rich pre-bloom conditions encountered in the present study. The very low bacterial production and respiration rates suggest that substrate must have been growth-limiting for the bacterial community. The significant correlation of BA with chl *a* and POC further suggests that bacterial accumulation was closely tied to sources of substrate.

Consequently, the cytological characteristics of the bacterial population support the view that the system in Fram Strait had entered the early spring phase, in which bacteria most probably experienced reduced grazing pressure but were still limited by substrate.

Inferred trophic relationships and possible advantages of mixotrophy

The microbial food web encountered in Fram Strait appeared trophically balanced despite an overall low NCP (Fig. 6). The balance of large heterotrophs with their potential prey is further suggested by the data in Fig. 7, which were plotted according to the method used by Suzuki & Miyabe (2007). Based on volumetric measurements of the stocks and physiological consid-

erations, Suzuki & Miyabe (2007) suggested that heterotrophic ciliates and their prey are in trophic balance when data points fall between the 2 theoretical lines indicating the outer boundaries for ciliate growth. Thus, both the carbon flow, calculated from literature growth rates (Fig. 6), and volumetric predator–prey considerations (Fig. 7), suggest a balanced microbial food web in Fram Strait, despite the low abundance of microbes certainly impacted predator–prey interactions due to decreased encounter rates (Lessard & Murrell 1998, Sherr & Sherr 2009).

Interestingly, the ciliate community was dominated by chloroplast-bearing forms, such as *Myrionecta* sp. (Stoecker et al. 1991, Hansen & Fenchel 2006), *Laboea strobila* and *Strombidium conicum* (Stoecker & Michaels 1991). There is some evidence that chloroplast-retaining ciliates may dominate in oligotrophic situations (Stoecker et al. 1989), which may indicate that, in a relatively food-poor environment such as in Fram Strait, it is an advantage not to base one's nutri-
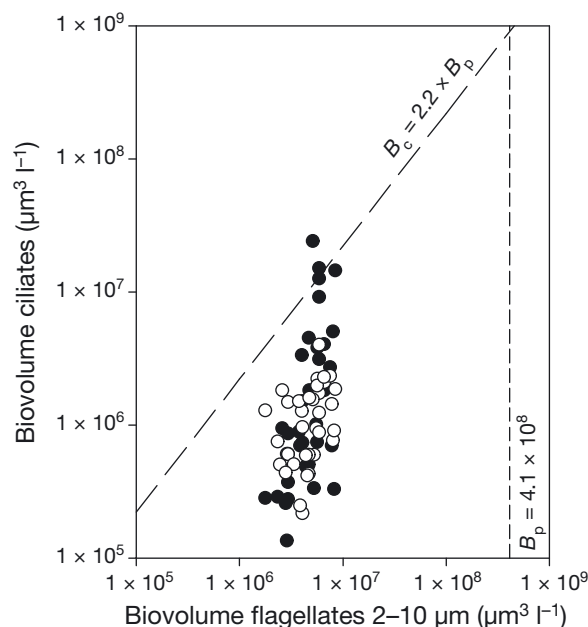

Fig. 7. Biovolume of flagellates <10 μm and ciliates (○: heterotrophic ciliates; ●: mixotrophic ciliates). The equilibrium between the food requirements of the ciliates and the production of their potential prey (here, both phototrophic and heterotrophic flagellates <10 μm) is assessed by the 2 broken lines. According to Suzuki & Miyabe (2007), the inclined broken line ($B_c = 2.2 \times B_p$) indicates the feasible equilibrium between prey production and ciliate food demands, while the vertical broken line indicates the lower limit of prey biovolume ($B_p = 4.1 \times 10^8$ μm l^{-1}) to sustain the minimal food demands of the ciliates. Points falling onto the broken lines suggest ciliates being controlled by the amount of prey (bottom-up), while points grouped between the theoretical boundaries imply an equilibrium between ciliates and their potential prey

tion on phagotrophy alone. Indeed, according to Fig. 7, mixotrophic ciliate volume was not always balanced by the volume of potential prey (filled circles crossing the line), suggesting that mixotrophs could most probably not have survived exclusively by heterotrophy.

The large proportion of plastidic ciliates raises questions about the contribution of ciliates to chl a and primary production, and ultimately their role in carbon and nutrient transfer to higher trophic levels. Putt (1990) found that ciliates in the Nordic Seas contribute up to 15% of the total chl a, while Stoecker et al. (1989) estimated that ciliates account for about 9% of chl a on Georges Bank. Calculations using published values on ciliate chl a content (Putt 1990 for *Laboea* sp. and *Strombidium* spp., Stoecker et al. 1991 for *Mesodinium rubrum*), suggest that plastidic ciliates could potentially have contributed between 1 and 26% of total chl a (average 7%). The contribution of these ciliates to primary production is unknown. Stoecker et al. (1989) reported, however, that *M. rubrum* at abundances similar to those reported from Fram Strait (order of 10^2 to 10^3 cells l^{-1}) accounted for up to 6% of total primary production in the surface waters of Georges Bank. Further, it is noteworthy that most of the chloroplast-bearing ciliates in Fram Strait were large (*M. rubrum* 8913 ± 6592 μm^3, mixotrophic ciliates $65\,545 \pm 70\,202$ μm^3) and were thus probably more phototrophic than smaller specimens because the volume-specific respiration rate decreases with increasing cell size (Fenchel & Finlay 1983). It is thus likely that plastidic ciliates had an advantageous effect on the productivity of the ecosystem in Fram Strait. Enhanced system productivity due to mixotrophy has also been demonstrated by modelling and has been argued to have a significant positive effect on the ecosystem's stability (Hammer & Pitchford 2005). Thus, phototrophs from small flagellates to large plastidic ciliates may have contributed profoundly to the structure and production of the system encountered in Fram Strait.

CONCLUSION

This study from Fram Strait in early spring shows that, despite a heavy cover of sea ice, light penetrated deeply into the water column wherever leads were formed between the ice floes. This allowed phototrophic growth to occur, as indicated by (1) the dominance of phototrophic protists ($H_{protist}$:P < 1) and (2) positive net community production (NCP >> 0) at most stations. Small phototrophs formed the basis of the microbial food web, most likely releasing the bacterial community from grazing pressure and allowing for the accumulation of a large bacterial biomass despite very low BP. The data presented here are among the few

descriptions of an Arctic marine ecosystem in its pre-bloom stage. The structural complexity of the microbial community we encountered, and its positive net community production, call for an increased research effort in order to understand the functioning and biogeochemical balance of Arctic marine ecosystems during seasons other than the late spring and summer months.

LITERATURE CITED

Agawin NSR, Duarte CM, Agustí S (2000) Nutrient and temperature control of the contribution of picoplankton to phytoplankton biomass and production. Limnol Oceanogr 45:591–600

Alonso-Sáez L, Sánchez O, Gasol JM, Balagué V, Pedrós-Alio C (2008) Winter-to-summer changes in the composition and single-cell activity of near-surface Arctic prokaryotes. Environ Microbiol 10:2444–2454

Anderson L (2002) DOC in the Arctic Ocean. In: Hansell D, Carlsson L (eds) Biogeochemistry of marine dissolved organic matter. Academic Press, San Diego, CA, p 665–683

Anderson MR, Rivkin RB (2001) Seasonal patterns in grazing mortality of bacterioplankton in polar oceans: a bipolar comparison. Aquat Microb Ecol 25:195–206

Arrigo KR (2005) Marine microorganisms and global nutrient cycles. Nature 437:349–355

Ashjian C, Smith S, Bignami F, Hopkins T, Lane P (1997) Distribution of zooplankton in the Northeast Water Polynya during summer 1992. J Mar Syst 10:279–298

Auf dem Venne H (1994) Zur Verbreitung und ökologischen Bedeutung planktischer Ciliaten in zwei verschiedenen Meeresgebieten: Grönlandsee und Ostsee. Ber Sonderforschungsbereich 313. Univ Kiel 33:1–109

Azam F, Fenchel T, Field JG, Gray JS, Meyer-Reil LA, Thingstad F (1983) The ecological role of water-column microbes in the sea. Mar Ecol Prog Ser 10:257–263

Behrenfeld MJ (2010) Abandoning Sverdrup's Critical Depth Hypothesis on phytoplankton blooms. Ecology 91:977–989

Belzile C, Brugel S, Nozais C, Gratton Y, Demers S (2008) Variations of the abundance and nucleic acid content of heterotrophic bacteria in Beaufort Shelf waters during winter and spring. J Mar Syst 74:946–956

Bloem J, Bär-Gilissen MJB, Cappenberg TE (1986) Fixation, counting, and manipulation of heterotrophic nanoflagellates. Appl Environ Microbiol 52:1266–1272

Booth BC, Smith WO (1997) Autotrophic flagellates and diatoms in the Northeast Water Polynya, Greenland: summer 1993. J Mar Syst 10:241–261

Calbet A, Landry MR (2004) Phytoplankton growth, microzooplankton grazing, and carbon cycling in marine systems. Limnol Oceanogr 49:51–57

Carritt D, Carpenter J (1996) Comparison and evaluation of

currently employed modifications of Winkler method for determining dissolved oxygen in seawater — a Nasco report. J Mar Res 24:286–318

Cole JJ, Findlay S, Pace ML (1988) Bacterial production in fresh and saltwater ecosystems: a cross-system overview. Mar Ecol Prog Ser 43:1–10

del Giorgio PA, Cole JJ (1998) Bacterial growth efficiency in natural aquatic systems. Annu Rev Ecol Syst 29:503–541

Ducklow H (2003) Seasonal production and bacterial utilization of DOC in the Ross Sea, Antarctica. In: DiTullio GR, Dunbar RB (eds) Biochemistry of the Ross Sea, Vol Antarctic Res Ser, vol 78, Washington, DC, p 143–158

Ducklow HW, Carlson CA (1992) Oceanic bacterial production. Adv Microb Ecol 12:113–181

Engbrodt R, Kattner G (2005) On the biogeochemistry of dissolved carbohydrates in the Greenland Sea (Arctic). Org Geochem 36:937–948

Fenchel T, Finlay BJ (1983) Respiration rates in heterotrophic, free-living protozoa. Microb Ecol 9:99–122

Garneau MÈ, Roy S, Lovejoy C, Gratton Y, Vincent WF (2008) Seasonal dynamics of bacterial biomass and production in a coastal arctic ecosystem: Franklin Bay, western Canadian Arctic. J Geophys Res 113:C07S91 doi:10.1029/2007JC004281

Gasol JM, del Giorgio PA, Duarte CM (1997) Biomass distribution in marine planktonic communities. Limnol Oceanogr 42:1353–1363

Gradinger RR, Baumann MEM (1991) Distribution of phytoplankton communities in relation to the large-scale hydrological regime in the Fram Strait. Mar Biol 111:311–321

Gradinger R, Lenz J (1995) Seasonal occurrence of picocyanobacteria in the Greenland Sea and central Arctic Ocean. Polar Biol 15:447–452

Hammer AC, Pitchford JW (2005) The role of mixotrophy in plankton bloom dynamics, and the consequences for productivity. ICES J Mar Sci 62:833–840

Hansen PJ, Fenchel T (2006) The bloom-forming ciliate *Mesodinium rubrum* harbours a single permanent endosymbiont. Mar Biol Res 2:169–177

Hansen PJ, Bjørnsen PK, Hansen BW (1997) Zooplankton grazing and growth: scaling within the 2 to 2000 µm body size range. Limnol Oceanogr 42:687–704

Hop H, Falk-Petersen S, Svendsen H, Kwasniewski S, Pavlov V, Pavlova O, Søreide JE (2006) Physical and biological characteristics of the pelagic system across Fram Strait to Kongsfjorden. Prog Oceanogr 71:182–231

Howard-Jones MH, Ballard VD, Allen AE, Frischer ME, Verity PG (2002) Distribution of bacterial biomass and activity in the marginal ice zone of the central Barents Sea during summer. J Mar Syst 38:77–91

Karayanni H, Christaki U, Van Wambeke F, Thyssen M, Denise M (2008) Heterotrophic nanoflagellate and ciliate bacterivorous activity and growth in the northeast Atlantic Ocean: a seasonal mesoscale study. Aquat Microb Ecol 51:169–181

Kirchman DL, Malmstrom RR, Cottrell MT (2005) Control of bacterial growth by temperature and organic matter in the Western Arctic. Deep-Sea Res II 52:3386–3395

Kirchman DL, Elifantz H, Dittel A, Malmstrom R, Cottrell MT (2007) Standing stocks and activity of Archaea and Bacteria in the western Arctic Ocean. Limnol Oceanogr 52:495–507

Lara RJ, Kattner G, Tillmann U, Hirche HJ (1994) The North East Water polynya (Greenland Sea) II. Meachanisms of nutrient supply and influence on phytoplankton distribution. Polar Biol 14:483–490

Lee S, Fuhrman JA (1987) Relationships between biovolume and biomass of naturally derived marine bacterioplankton. Appl Environ Microbiol 53:1298–1303

Lessard EJ, Murrell MC (1998) Microzooplankton herbivory and phytoplankton growth in the northwestern Sargasso Sea. Aquat Microb Ecol 16:173–188

Levinsen H, Nielsen TG, Hansen BW (2000) Annual succession of marine pelagic protozoans in Disko Bay, West Greenland, with emphasis on winter dynamics. Mar Ecol Prog Ser 206:119–134

Lovejoy C, Massana R, Pedrós-Alió C (2006) Diversity and distribution of marine microbial eukaryotes in the Arctic Ocean and adjacent seas. Appl Environ Microbiol 72:3085–3095

Lovejoy C, Vincent WF, Bonilla S, Roy S and others (2007) Distribution, phylogeny, and growth of cold-adapted picoprasinophytes in Arctic seas. J Phycol 43:78–89

Menden-Deuer S, Lessard EJ (2000) Carbon to volume relationships for dinoflagellates, diatoms, and other protist plankton. Limnol Oceanogr 45:569–579

Müller-Niklas G, Herndl GJ (1996) Dynamics of bacterioplankton during a phytoplankton bloom in the high Arctic waters of the Franz Joseph Land archipelago. Aquat Microb Ecol 11:111–118

Pesant S, Legendre L, Gosselin M, Bjornsen P, Fortier L, Michaud J, Nielsen TG (2000) Pathways of carbon cycling in marine surface waters: the fate of small-sized phytoplankton in the Northeast Water Polynya. J Plankton Res 22:779–801

Pomeroy LR, Deibel D (1986) Temperature regulation of bacterial activity during the spring bloom in Newfoundland coastal waters. Science 233:359–361

Porter KG, Feig YS (1980) The use of DAPI for identifying and counting aquatic microflora. Limnol Oceanogr 25:943–948

Putt M (1990) Abundance, chlorophyll content and photosynthetic rates of ciliates in the Nordic Seas during summer. Deep-Sea Res 37:1713–1731

Putt M, Stoecker DK (1989) An experimentally determined carbon:volume ratio for marine 'oligotrichous' ciliates from estuarine and coastal waters. Limnol Oceanogr 34:1097–1103

Rich J, Gosselin M, Sherr E, Sherr B, Kirchman DL (1997) High bacterial production, uptake and concentrations of dissolved organic matter in the Central Arctic Ocean. Deep-Sea Res II 44:1645–1663

Rivkin RB, Anderson MR, Lajzerowicz C (1996) Microbial processes in cold oceans. I. Relationship between temperature and bacterial growth rate. Aquat Microb Ecol 10:243–254

Rokkan Iversen K, Seuthe L (2011) Seasonal microbial processes in a high-latitude fjord (Kongsfjorden, Svalbard): I. Heterotrophic bacteria, picoplankton and nanoflagellates. Polar Biol 34:731–749

Rose JM, Caron DA (2007) Does low temperature constrain the growth rates of heterotrophic protists? Evidence and implications for algal blooms in cold waters. Limnol Oceanogr 52:886–895

Rozanska M, Gosselin M, Poulin M, Wiktor JM, Michel C (2009) Influence of environmental factors on the development of bottom ice protist communities during the winter–spring transition. Mar Ecol Prog Ser 386:43–59

Sakshaug E (2004) Primary and secondary production in the Arctic seas. In: Stein R, Macdonald R (eds) The organic carbon cycle in the Arctic Ocean. Springer, Berlin, p 57–81

Sala MM, Terrado R, Lovejoy C, Unrein F, Pedrós-Alió C (2008) Metabolic diversity of heterotrophic bacterioplankton over winter and spring in the coastal Arctic Ocean. Environ Microbiol 10:942–949

Sanders RW, Porter KG, Bennett SJ, DeBiase AE (1989) Seasonal patterns of bacterivory by flagellates, ciliates, rotifers, and cladocerans in a freshwater planktonic community. Limnol Oceanogr 34:673–687

Sanders RW, Caron DA, Berninger UG (1992) Relationships between bacteria and heterotrophic nanoplankton in marine and freshwaters: an inter-ecosystem comparsion. Mar Ecol Prog Ser 86:1–14

Schlichtholz P, Houssais MN (2002) An overview of the theta-S correlations in Fram Strait based on the MIZEX 84 data. Oceanologia 44:243–272

Seuthe L, Darnis G, Wexels Riser C, Wassmann P, Fortier L (2007) Winter–spring feeding and metabolism of Arctic copepods: insights from faecal pellet production and respiration measurements in the southeastern Beaufort Sea. Polar Biol 30:427–436

Seuthe L, Rokkan Iversen K, Narcy F (2011) Microbial processes in a high-latitude fjord (Kongsfjorden, Svalbard): II. Ciliates and dinoflagellates. Polar Biol 34:751–766

Sherr BF, Sherr EB (2003) Community respiration/production and bacterial activity in the upper water column of the central Arctic Ocean. Deep-Sea Res I 50:529–542

Sherr EB, Sherr BF (2009) Capacity of herbivorous protists to control initiation and development of mass phytoplankton blooms. Aquat Microb Ecol 57:253–262

Sherr EB, Sherr BF, Fessenden L (1997) Heterotrophic protists in the central Arctic Ocean. Deep-Sea Res II 44:1665–1682

Sherr EB, Sherr BF, Wheeler PA, Thompson K (2003) Temporal and spatial variation in stocks of autotrophic and heterotrophic microbes in the upper water column of the central Arctic Ocean. Deep-Sea Res I 50:557–571

Simon M, Azam F (1989) Protein content and protein synthesis rates of planktonic marine bacteria. Mar Ecol Prog Ser 51:201–213

Skoog A, Wedborg M, Lara R, Kattner G (2005) Spring distribution of dissolved organic matter in a system encompassing the Northeast Water Polynya: implications for early-season sources and sinks. Mar Chem 94:175–188

Smith D, Azam F (1992) A simple, economical method for measuring bacterial protein synthesis rates in seawater using ^{3}H-leucine. Mar Microb Food Webs 6:107–114

Sorokin YI (1971) Abundance and production of bacteria in open water of central Pacific. Oceanol Acad Sci USSR 11:89–94

Stoecker DK, Michaels AE (1991) Respiration, photosynthesis and carbon metabolism in planktonic ciliates. Mar Biol 108:441–447

Stoecker DK, Taniguchi A, Michaels AE (1989) Abundance of autotrophic, mixotrophic and heterotrophic planktonic ciliates in shelf and slope waters. Mar Ecol Prog Ser 50:241–254

Stoecker DK, Putt M, Davis LH, Michaels AE (1991) Photosynthesis in *Mesodinium rubrum*: species-specific measurements and comparison to community rates. Mar Ecol Prog Ser 73:245–252

Sturluson M, Nielsen TG, Wassmann P (2008) Bacterial abundance, biomass and production duringspring blooms in the northern Barents Sea. Deep-Sea Res II 55:2186–2198

Suzuki T, Miyabe C (2007) Ecological balance between ciliate plankton and its prey candidates, pico- and nanoplankton, in the East China Sea. Hydrobiologia 586:403–410

Terrado R, Lovejoy C, Massana R, Vincent WF (2008) Microbial food web responses to light and nutrients beneath the coastal Arctic Ocean sea ice during the winter–spring transition. J Mar Syst 74:964–977

Thingstad TF, Martinussen I (1991) Are bacteria active in the cold pelagic ecosystem of the Barents Sea? Polar Res 10: 255–266

Tremblay G, Belzile C, Gosselin M, Poulin M, Roy S, Tremblay JÉ (2009) Late summer phytoplankton distribution along a 3500 km transect in Canadian Arctic waters: strong numerical dominance by picoeukaryotes. Aquat Microb Ecol 54:55–70

Vaqué D, Guadayol Ò, Peters F, Felipe J and others (2008) Seasonal changes in planktonic bacterivory rates under the ice-covered coastal Arctic Ocean. Limnol Oceanogr 53:2427–2438

Vernet M, Matrai PA, Andreassen I (1998) Synthesis of particulate and extracellular carbon by phytoplankton at the marginal ice zone in the Barents Sea. J Geophys Res 103:1023–1037

von Quillfeldt CH (1997) Distribution of diatoms in the Northeast Water Polynya, Greenland. J Mar Syst 10:211–240

von Quillfeldt CH (2000) Common diatom species in arctic spring blooms: their distribution and abundance. Bot Mar 43:499–516

Wells LE, Deming JW (2003) Abundance of bacteria, the *Cytophaga-Flavobacterium* cluster and Archaea in cold oligotrophic waters and nepheloid layers of the Northwest Passage, Canadian Archipelago. Aquat Microb Ecol 31: 19–31

Wheeler PA, Gosselin M, Sher E, Thibault D, Kirchman DL, Benner R, Whitledge TE (1996) Active cycling of organic carbon in the central Arctic Ocean. Nature 380:697–699

Williams PJB, Raine RCT, Bryan JR (1979) Agreement between the C-14 and oxygen methods of measuring phytoplankton production—reassessment of the photosynthetic quotient. Oceanol Acta 2:411–416

Yager PL, Connelly TL, Mortazavi B, Wommack KE and others (2001) Dynamic bacterial and viral response to an algal bloom at subzero temperatures. Limnol Oceanogr 46: 790–801